PAPER

Comparison of runaway electron generation parameters in small, medium-sized and large tokamaks—A survey of experiments in COMPASS, TCV, ASDEX-Upgrade and JET

To cite this article: V.V. Plyusnin *et al* 2018 *Nucl. Fusion* **58** 016014

IOP Publishing | International Atomic Energy Agency Nuclear Fusion

Nucl. Fusion **58** (2018) 016014 (15pp) https://doi.org/10.1088/1741-4326/aa8f05

Comparison of runaway electron generation parameters in small, medium-sized and large tokamaks—A survey of experiments in COMPASS, TCV, ASDEX-Upgrade and JET

V.V. Plyusnin[1], C. Reux[2], V.G. Kiptily[3], G. Pautasso[4], J. Decker[5], G. Papp[4], A. Kallenbach[4], V. Weinzettl[6], J. Mlynar[6], S. Coda[5], V. Riccardo[3], P. Lomas[3], S. Jachmich[7], A.E. Shevelev[8], B. Alper[3], E. Khilkevitch[8], Y. Martin[5], R. Dux[4], C. Fuchs[4], B. Duval[5], M. Brix[3], G. Tardini[4], M. Maraschek[4], W. Treutterer[4], L. Giannone[4], A. Mlynek[4], O. Ficker[6], P. Martin[9], S. Gerasimov[3], S. Potzel[4], R. Paprok[6], P. J. McCarthy[10], M. Imrisek[6], A. Boboc[3], K. Lackner[4], A. Fernandes[1], J. Havlicek[6], L. Giacomelli[11], M. Vlainic[12], M. Nocente[11,13], U. Kruezi[3], COMPASS team[6], TCV team[5], ASDEX-Upgrade team, EUROFusion MST1 Team[a] and JET contributors[b]

EUROFusion Consortium, JET, Culham Science Centre, Abingdon, OX14 3DB, United Kingdom
[1] Instituto de Plasmas e Fusão Nuclear, Instituto Superior Tecnico, Universidade de Lisboa, Lisboa, Portugal
[2] CEA, IRFM, F-13108 Saint-Paul-lez-Durance, France
[3] CCFE, Culham Science Centre, Abingdon, OX14 3DB, United Kingdom
[4] Max-Planck-Institut für Plasmaphysik, Garching D-85748, Germany
[5] Swiss Plasma Centre, EPFL, CH-1015 Lausanne, Switzerland
[6] IPP AS CR, Za Slovankou 3, CZ-18200 Prague, Czechia
[7] Laboratoire de Physique des Plasmas-Laboratorium voor Plasmafysica, ERM/KMS, B-1000 Brussels, Belgium
[8] Ioffe Institute, St. Petersburg, 194021, Russian Federation
[9] Consorzio RFX, corso Stati Uniti 4, 35127 Padova, Italy
[10] Department of Physics, University College Cork, Cork, Ireland
[11] Istituto di Fisica del Plasma, CNR, Milano, Italy
[12] Department of Applied Physics, Ghent University, Sint-Pietersnieuwstraat 41, Technicum B4, Ghent B-9000, Belgium
[13] Dipartimento di Fisica 'G. Occhialini', Università di Milano-Bicocca, Milano, Italy

E-mail: vladislav.plyusnin@ipfn.ist.utl.pt

Received 17 January 2017, revised 6 August 2017
Accepted for publication 26 September 2017
Published 8 November 2017

Abstract

This paper presents a survey of the experiments on runaway electrons (RE) carried out recently in frames of EUROFusion Consortium in different tokamaks: COMPASS, ASDEX-Upgrade, TCV and JET. Massive gas injection (MGI) has been used in different scenarios for RE generation in small and medium-sized tokamaks to elaborate the most efficient and reliable ones for future RE experiments. New data on RE generated at disruptions in COMPASS and ASDEX-Upgrade was collected and added to the JET database. Different accessible parameters of disruptions, such as current quench rate, conversion rate of plasma current into

[a] See the author list of [59].
[b] See the author list of [60].

runaways, etc have been analysed for each tokamak and compared to JET data. It was shown, that tokamaks with larger geometrical sizes provide the wider limits for spatial and temporal variation of plasma parameters during disruptions, thus extending the parameter space for RE generation. The second part of experiments was dedicated to study of RE generation in stationary discharges in COMPASS, TCV and JET. Injection of Ne/Ar have been used to mock-up the JET MGI runaway suppression experiments. Secondary RE avalanching was identified and quantified for the first time in the TCV tokamak in RE generating discharges after massive Ne injection. Simulations of the primary RE generation and secondary avalanching dynamics in stationary discharges has demonstrated that RE current fraction created via avalanching could achieve up to 70–75% of the total plasma current in TCV. Relaxations which are reminiscent the phenomena associated to the kinetic instability driven by RE have been detected in RE discharges in TCV. Macroscopic parameters of RE dominating discharges in TCV before and after onset of the instability fit well to the empirical instability criterion, which was established in the early tokamaks and examined by results of recent numerical simulations.

Keywords: Tokamak, disruptions, runaway electrons, hard x rays

(Some figures may appear in colour only in the online journal)

1. Introduction

Disruptive termination of plasma discharges is one of the most critical issues for tokamak operations. International thermonuclear experimental reactor (ITER) is based on the tokamak concept [1, 2]. Together with excessive electromagnetic forces and heat loads onto plasma facing components (PFC) the major disruption in tokamaks causes an induction of strong electric fields occurring during thermal quench (TQ) and plasma current decay stage—current quench (CQ). If these electric fields are strong enough to overcome the dissipative effect of the Coulomb collisions, they accelerate plasma electrons into runaway regime [3–7]. Such runaway electrons (RE) will be accelerated ever more rapidly because the dissipative collisional friction decreases with increase of electron velocity. Unlimited acceleration will inevitably lead to the relativistic energies acquired by RE.

Major disruptions in tokamaks often resulted in generation of large populations of high-energy RE. Large number of spontaneous and intentional major disruptions in the JET tokamak led to generation of RE beams with the energies from several MeV till to several tens of MeV and current values sometimes exceeding 2.5 MA [8–13]. Generation of intense RE beams with relativistic energies has been detected during major disruptions in TORE Supra [14], JT-60U [15] and TFTR [16]. The density of RE generated during disruptions in these large tokamaks was high enough to create post-disruption current plateaux with values up to 60–70% of the pre-disruptive plasma currents [11]. Such intense RE beams constitute a serious problem for the safety operation of tokamaks since the interaction of these beams with surrounding PFC resulted in high heat loads, sputtering and melting of the first wall materials. In TORE Supra the RE beam damaged the actively cooled limiter and caused the water leak into vacuum vessel [14]. Experimental trend in disruption generated RE [11] suggests that ITER disruptions could generate much higher RE currents resulting in much severe consequences when relativistic RE beams will interact with the first wall.

Significant efforts in theoretical studies and numerical modelling of the RE generation during disruptions have been done to investigate the trend in this process toward the domain of ITER operational parameters ([1, 2] and references cited therein). The main mechanism responsible for generation of large RE currents during disruptions in ITER is considered to be an avalanching of secondary RE. These secondary RE are generated due to close distance electron–electron collisions between existing seed RE and thermal electrons, thus the latter become runaway [17–19]. The RE avalanching is not possible without the RE seeds that can exist in pre-disruptive plasmas, or they can be produced due to several processes during TQ and CQ [9–11, 20].

The first known source for seed RE is the Dreicer acceleration [4–7]. Performed in recent decades studies allowed characterization of other mechanisms, which could be responsible for the creation of RE seeds, in addition to the Dreicer generation. One of such mechanisms is hot tail runaway generation [21–23]. The energetic particles in the tail of initial distribution function of high temperature plasma need longer time to slow down than those in low energy part of the distribution if the plasma cools down sufficiently fast. These energetic particles constitute a hot tail of the mainly cold post-TQ electron distribution. Due to the increase of electric fields in TQ and CQ a significant part of this hot tail can be converted into RE.

Also, it was pointed out that even a small sources, such as the tritium decay and Compton scattering of γ-rays emitted by activated wall on plasma electrons, would be sufficient to generate significant RE populations during CQ [24]. In [25] it was shown, that interaction of high energy RE with the first wall also could cause an additional yield of the high-energy electrons (with MeV energies) from surrounding surfaces.

Simulations of runaway process, which might occur at major disruptions in ITER without mitigation, demonstrate

the possibility to generate RE currents with up to 10 MA in multi-MeV energy range (for example [26]). Localized interaction of such intense RE beams with surrounding surfaces inevitably will result in inacceptable loads and evaporation of the Be first wall [27]. Therefore, in the tokamak-reactor, such as ITER, the generation of RE is inacceptable.

To prevent detrimental consequences of disruptions and RE generation events the efficient methods for disruption mitigation and suppression/avoidance of runaway process are essential. Massive gas injection (MGI) is considered as a part for the prospective design of disruption mitigation system in ITER (ITER-DMS) to suppress/avoid detrimental effects of major disruptions and generation of intense RE beams. Significant advances in experimental studies of MGI capabilities and characterization of the methods for the fast plasma shutdown have been achieved during recent years [28, 29]. Despite that MGI demonstrated the ability to mitigate a majority of severe processes caused by disruptions, a set of problems related to RE avoidance/suppression is still unresolved [12, 13]. To overcome existing problems a detailed knowledge of runaway generation physics and improved models for simulation of interaction of RE beams with large quantities of injected impure gases are required.

This paper presents a survey of the first series of experiments on RE generation carried out in frames of EUROFusion Consortium program [30–32] in small and medium-sized (MST) European tokamaks—in COMPASS, TCV and ASDEX-Upgrade. Results of these experiments have been analysed in comparison to the data collected in experiments on RE generation carried out in JET with PFC made from carbon (JET-C) and in JET with ITER-like wall (JET-ILW).

In one group of experiments the parameters of disruption generated RE have been studied depending on increase of the device experimental parameters: magnetic field (B_0), plasma current (I_{pl}), etc. The RE data collected in ASDEX-Upgrade and COMPASS was included into database elaborated in experiments on disruptions and RE in JET-C and JET-ILW [11, 25, 33]. A detailed analysis was dedicated to study of the RE parameters evolution depending on geometrical sizes of tokamak experiments. This analysis has demonstrated conformity of the recent results from small and medium sized tokamaks [30–32] to the data on RE obtained earlier in large tokamaks [11–13, 25, 33].

Another part of experiments was dedicated to the study of RE generation parameters in stationary tokamak discharges. A scenario of RE generation under stationary conditions constitutes the subject of a special attention due to the convenient possibility to measure reliably the plasma parameters during onset, growth and loss of relativistic RE [34, 35]. This stationary RE generation scenario was developed in experiments with low plasma density on COMPASS and TCV. Using the measured plasma parameters the RE generation dynamics was quantified in frames of conventional theory of runaways. Obtained data was compared to the data collected in the JET stationary RE discharge [35]. Parameters of the observed RE generation events, such as critical fields and energies, have been analysed to highlight the differences and similarities of RE generation in low-density and moderate density plasmas. MGIs into stationary RE discharges in TCV and COMPASS were used for establishing the operational regimes for future experiments on the RE beam dissipation. RE avalanche events after MGI into RE discharges have been detected and studied in TCV. The events associated to the kinetic instability driven by RE have been observed and studied in TCV. Obtained results are in adequate conformity with the statements formulated in frames of the theory for kinetic instability driven by relativistic RE.

2. Diagnostics for RE detection and measurements of RE parameters

Relativistic RE interacting with background plasma and neutrals produce a bremsstrahlung hard x-ray emission (HXR) in the sub-MeV and MeV energy ranges. Also RE produce γ-radiation and photo-neutrons hitting the elements of PFC. Measurements of these radiations in different time points and subsequent numerical processing of the obtained data provide the information on different RE parameters, such as mean and maximum energies of RE populations, their spatial locations, etc.

The HXR detectors are used to register the RE generation in the ASDEX-Upgrade disruption experiments. The neutron spectrometry diagnostic used on ASDEX-Upgrade has demonstrated that maximal energy of RE in disruptions has reached up to ≈10 MeV.

In JET the HXR emission is measured with the set of horizontally and vertically viewing NaI(Tl), Bi_4GeO_{12} (usually referred as BGO) and $LaBr_3$ spectrometers. The JET neutron/γ-emission profile monitor with highly collimated detectors is routinely used for neutron and γ-rays measurements. These diagnostics allow the measurements of spatial distribution of HXR emission sources in the JET plasma cross-section. The data from vertically viewing HXR spectrometer on JET has been numerically processed using the DeGaSum code [36] to study the evolution of the RE distribution function (REDF) in disruptions and during the stationary discharge. Reconstruction of REDF from the measured HXR spectra revealed the generation of RE population with maximal energies up to ≈7–8 MeV and with mean energy ≈2.5–3 MeV in stationary discharge [35]. Similar or even higher mean RE energies were measured in JET-ILW disruptions [12, 13, 33]. The maximum RE energy in disruptions reached up to 12–15 MeV (sometimes up to 20–25 MeV) [25, 33]. A detailed analysis of the RE parameters inferred on the basis of HXR spectrometry and other methods could be found in [8, 11, 25, 33, 36]. The HXR bremsstrahlung, which is radiated following the relativistic electrons scattering on the background plasma ions, is characterized by very narrow forward radiation pattern with angular half-width about of $\theta \sim 1/\gamma_0$, (γ_0 is relativistic parameter of energetic electrons). Two narrow radiation patterns with angular half-size $\theta \approx 0.06$–0.1 have been detected by vertical and horizontal HXR cameras in JET [35] indicating that maximum energies of electrons scattered on background ions could be $W_{max} \approx 5$–8 MeV. One can see that angular characteristics of the measured HXR radiation

and the processed data from the HXR spectroscopy yielded similar values on RE energy allowing cross-verification.

On TCV a photo-multiplier tube for Hard x-rays (PMTX) is routinely used for measurements of the HXR emission and detection of RE generation. This detector is placed outside the torus, in the machine hall. Due to the large production of energetic HXRs following the RE generation in stationary discharges or during post-disruption RE plateaux the other HXR diagnostics (with energy thresholds ≈20 keV and ≈200 keV) usually saturate and only the PMTX camera could be effectively used for detection of RE generation regimes.

Two NaI(Tl) scintillation detectors with photomultipliers for HXR measurements were used during RE experiments in COMPASS. Since these detectors are not shielded, they are characterized by the energy threshold ≈50 keV. Also for measurements of HXR a detector based on ZnS(Ag) scintillator with photomultiplier was used. This detector was shielded with 10 cm of lead. The distance of both detectors from the tokamak main axis is ≈4 m. A detailed description of the diagnostics used in COMPASS experiments also could be found elsewhere [31]. During the RE dominated discharges in COMPASS the synchrotron radiation from RE beam was directly measured by an infrared camera [37].

3. RE generated during disruptions in Tokamaks

Series of experiments in ASDEX-Upgrade and COMPASS have been carried out in order to design the reliable scenario of disruptions with RE generation and to create the basis for future experiments on RE studies in small and medium-sized tokamaks. Disruption scenarios with RE generation in both tokamaks are based on the MGI disruption scenario developed in JET for RE studies [12, 13]. In JET the disruption mitigation valves (DMVs) have been used for injection of Ar, Ne, Xe and Kr. This scenario is described in detail elsewhere [12, 13]. Similarly to JET, the fast injections of large amount of impure gases have been used to trigger the disruptions in limiter configurations in ASDEX-Upgrade and COMPASS [30–32].

The sequence of events in disruptions triggered by MGI is similar to those caused by constant gas puff [10, 11], but occurring in significantly shorter time. These processes are well known and their detailed phenomenological and quantitative descriptions can be found in many publications [9–13, 24, 33, 38]. The main characteristics are: after MGI the plasma develops strong MHD activity; The growth of MHD modes enables penetration of the impurity gas into plasma centre; This process resulted in the cooling of plasma core and formation of the hollow electron temperature profiles [11, 38]. Following these phases the complete plasma energy collapse occurs very quickly.

The RE generation scenario in ASDEX-Upgrade is based on L-mode Ohmic circular plasma discharges with inner limiter ($R_0 = 1.65$ m, $a_{pl} = 0.5$ m) and $I_{pl} \leqslant 0.8$ MA at $B_0 = 2.5$ T. The injection of 0.05–0.2 bar·l of Ar from the piezo-electric in-vessel valve resulted in characteristic rise of MHD activity and disruptions [30]. To optimize the RE generation at disruptions the low-density plasmas ($\langle n_e \rangle \approx (2.5\text{–}3.6) \cdot 10^{19}$ m^{-3})

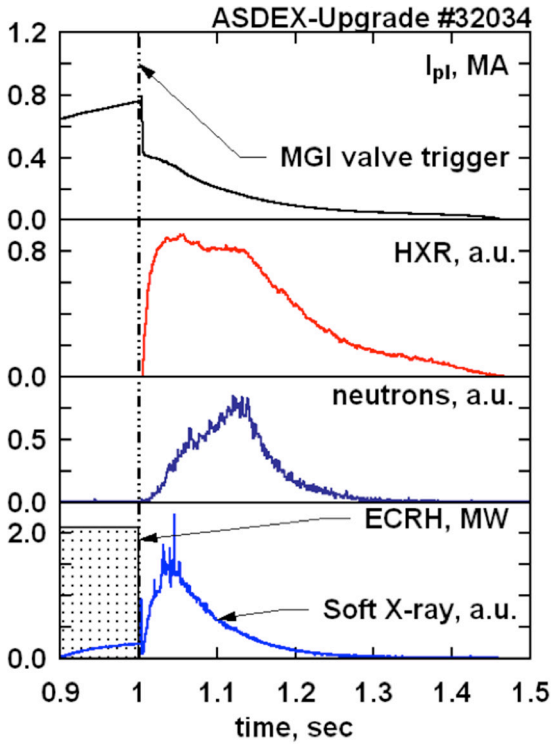

Figure 1. ASDEX-Upgrade discharge #32034: scenario for study RE generation at disruptions; disruption was induced by MGI triggered at $t = 1.0$ s (vertical dash-dot line); disruption time is $t \approx 1.005$ s; rectangle pulse of 2.1 MW ECRH is indicated by dot-filled shape; plasma current time derivative maximum on CQ stage is ≈ -250 MA s^{-1}; ohmic CQ evolution fits well to decay function with characteristic e-folding time $t_{CQ} \approx 2.8$ ms; noticeable deviation of current plateau evolution from exponential decay well corresponds to detection of HXR emission.

were heated by 2–2.5 MW of ECRH applied for 0.1–0.2 s immediately before Ar/Ne injections. Disruptions were well reproducible with typical thermal quench time $t_{TQ} \approx 0.001$ s. Figure 1 presents an example of temporal evolution of plasma parameters in the scenario for study of RE generation during disruptions in ASDEX-Upgrade.

Disruption of the discharge #32034 was induced by MGI from the piezo-electric valve, which was triggered at $t = 1.0$ s (vertical dash-dot line in figure 1). Usually, major disruption occurs during small time after valve triggering (~4–10 ms, depending on the injected gas type and quantity). In this pulse the disruption occurred in ~5 ms after valve triggering. The maximum of plasma current time derivative on CQ stage was ≈ -250 MA s^{-1}. CQ evolution fits well to decay function with characteristic e-folding time $t_{CQ} \approx 2.8$ ms. Transition of the plasma current evolution from exponential decay into slow decaying plateau well coincides to the detection of HXR emission and photo-neutrons indicating the generation of RE with energies up to 10 MeV. RE current plateaux with up to 0.4 MA and duration up to 0.4 s have been measured in series of disruptions dedicated to the RE studies in ASDEX-Upgrade.

Disruptions in hydrogen plasmas in ASDEX-Upgrade resulted in RE plateaux comparable to those obtained in deuterium, while the slightly lower RE currents were achieved in helium. MGI from the second DMV (triggered on 70th ms

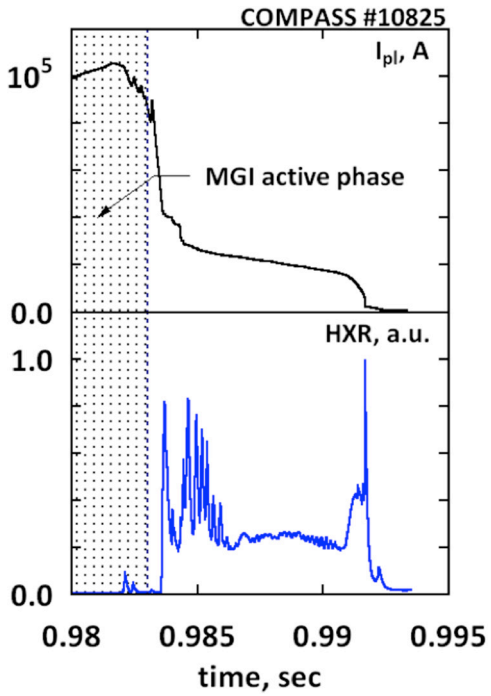

Figure 2. RE generation scenario in the COMPASS disruptions: RE plateau with ≈25–30 kA generated after disruption triggered by Ar injection in discharge #10825; MGI was triggered at $t = 0.98$ s; the injection active stage is indicated by filled area; disruption time is ≈0.983 s; plasma current time derivative maximum on CQ stage is ≈−130 MA s^{-1}; ohmic CQ evolution fits well to decay function with characteristic e-folding time $t_{CQ} \approx 0.5$ ms; noticeable deviation of current plateau evolution from exponential decay well corresponds to detection of HXR emission.

after the first injection) resulted in obvious suppressing effect on RE plateaux and allowed a study of dissipative effects of the MGI of high-Z gases on RE beams [30].

Similar scenario for RE generation studies has been developed in COMPASS: the circular plasma ($R_0 = 0.56$ m, $a_{pl} \approx 0.2$ m) with carbon limiter from the high field side (HFS) and additional one from the low field side (LFS) for the vessel protection [31]. Experimental magnetic field was $B_0 = 1.15$ T and plasma currents were $80 \leqslant I_{pl} \leqslant 140$ kA. An average electron density was kept relatively low ($\langle n_e \rangle \approx (0.8–2.2)\cdot 10^{19}$ m^{-3}) in order to maximize the RE generation rate.

Figure 2 presents an example of RE generation in COMPASS during disruption of pulse #10825. MGI was triggered at $t = 0.98$ s with the active injection phase lasted till to disruption event (≈0.003 s). The maximum of plasma current time derivative on CQ stage was ≈−130 MA s^{-1}. CQ evolutions in many disruptions fit well to decay function with characteristic e-folding time $t_{CQ} \approx 0.5$ ms. Detection of the HXR emission coincides to appearance of RE current plateau with value up to 30 kA. Sometimes the COMPASS disruptions resulted in RE current plateaux with values up to 60 kA. COMPASS data was added to the data on disruption generated RE in tokamaks.

The data on RE currents generated in tokamak disruptions shows an increasing trend with increase of the total plasma current from small and medium-sized devices toward JET (figure 3). The data plotted in figure 4 shows that the higher

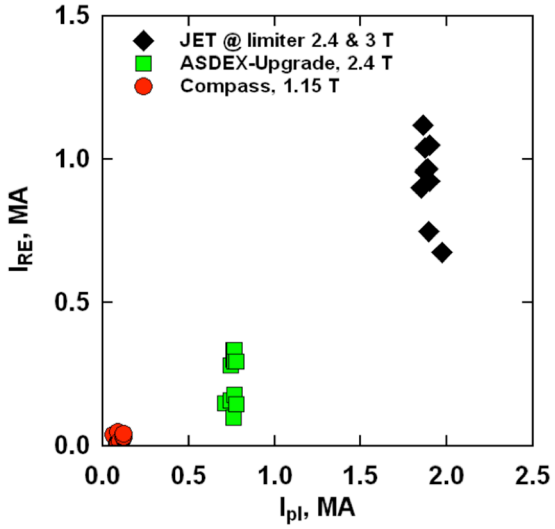

Figure 3. Disruption generated RE currents versus plasma currents in small, medium-sized and large tokamaks.

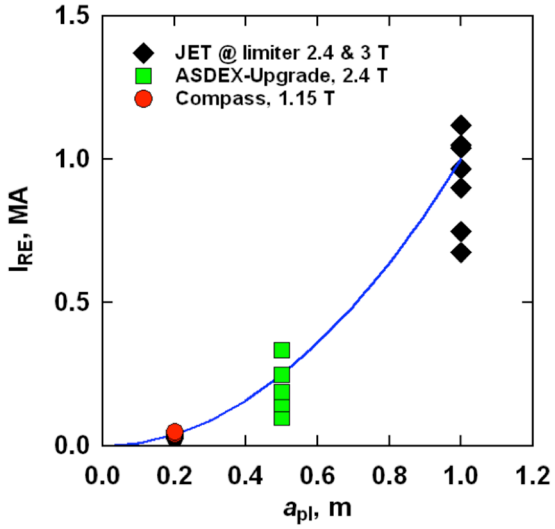

Figure 4. Generation of RE currents in COMPASS, ASDEX-Upgrade and JET depending on plasma minor radius; solid line represents a function of a_{pl}^2.

RE currents are generated in devices with the larger plasma minor radius ($I_{RE\_Ave} \propto a_{pl}^2$).

Figure 5 presents the data on RE generated in different tokamaks versus toroidal magnetic fields. In this Figure the data from smaller devices is added to the data on RE collected in JET-C and JET-ILW [11, 25, 33]. One can see, that values of RE plateaux measured in COMPASS disruptions at $B_0 = 1.15$ T and currents $I_{pl} \leqslant 120$ kA are similar to the JET data at $B_0 = 1.2$ T and currents 1 MA $\leqslant I_{pl} \leqslant 1.2$ MA. The MGI disruptions in ASDEX-Upgrade at current $I_{pl} \approx 0.8$ MA and $B_0 = 2.5$ T resulted in RE plateaux with values similar to those obtained in JET at $B_0 = 2–2.4$ T, but with pre-disruption plasma currents in JET at least two times higher: 1.4 MA $\leqslant I_{pl} \leqslant 2$ MA [11, 25, 33]. It is likely that maximum of RE current values generated in disruptions scales as a function, which is proportional to B_0^2. In figure 5 the dotted line represents the function $f(B_0) = \varepsilon_0^2 \cdot B_0^2$, where $\varepsilon_0 = a_{pl}/R_0 = 0.33$,

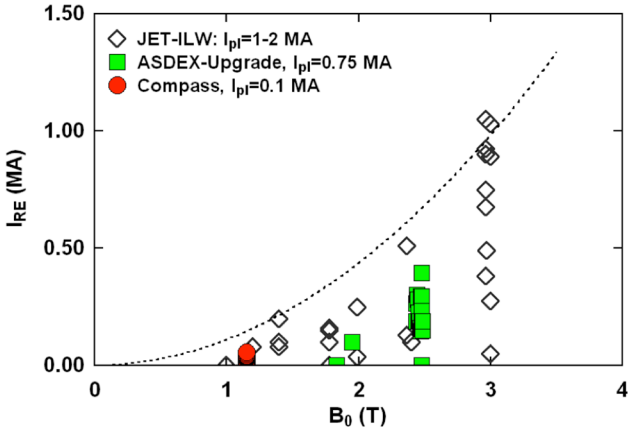

Figure 5. RE generation versus toroidal magnetic fields in small, medium-sized and large tokamaks (compare to data presented in figure 7 of [11]); dotted line represents a function of $\varepsilon_0^2 \cdot B_0^2$, where $\varepsilon_0 = a_{pl}/R_0 \approx 0.33$ as in JET (in COMPASS: $\varepsilon_0 = a_{pl}/R_0 \approx 0.35$; in ASDEX-Upgrade: $\varepsilon_0 = a_{pl}/R_0 \approx 0.303$).

which corresponds to the JET geometry sizes. Note, that ASDEX-Upgrade geometry provides $\varepsilon_0 = a_{pl}/R_0 \approx 0.303$ and for COMPASS case: $\varepsilon_0 = a_{pl}/R_0 \approx 0.36$. Generation of RE beams with the measured currents about of tens/hundreds kA at magnetic fields $B_0 = 1$–1.2 T in JET-ILW and COMPASS evidently indicates the absence of background for statements about existence of the threshold for RE generation on toroidal magnetic field value [2].

Maximum values of the RE current generated in ASDEX-Upgrade disruptions reached up to one half of pre-disruption plasma currents $\frac{I_{RE}}{I_{pl}} \leqslant 0.5$, while the RE current plateaux in COMPASS sometimes reached up to $\frac{I_{RE}}{I_{pl}} \approx 0.66$ of pre-disruption values (figure 6(*a*)). This data on conversion rate of plasma current into runaways is quite similar to the recent JET-ILW results confirming observed earlier apparent weak sensitivity of the current conversion rate versus I_{pl} values and geometrical sizes of experiments [11–13, 21, 22].

Unlike the current conversion rate, the CQ rate $I_\gamma = \frac{1}{I_{pl}} \frac{dI_{pl}}{dt}$ revealed strong dependence on the scale of experiments (figure 6(*b*)). The CQ process is usual driver for generation of high $E_{||}$—one of the determining factors for RE generation. In JET [11] the value of RE currents generated in disruptions has demonstrated almost linear dependence versus values of plasma current time derivatives ($\frac{dI_{pl}}{dt}$) evaluated on the beginning of CQ. From the CQ rate the average RE generation rate $\gamma_{RE} = \frac{1}{j_{RE}} \frac{dj_{RE}}{dt}$, where $j_{RE} = ecn_{RE}$, can be quantified when a measurable deviation of the plasma current from the exponential decay due to RE is detected, or even when RE plateaux are measured [11, 25, 33]. During RE plateau total plasma current is constant $I_{tot} = I_{pl} + I_{RE}$ and its time derivative is zero. Meanwhile, the plasma resistive current decays with characteristic e-folding time τ_{CQ} [8–13]. So that, $\frac{dI_{RE}}{dt} = -\frac{dI_{pl}}{dt}$ on the beginning of RE plateaux. Therefore, if the evolution of the plasma cross-section during CQ is known from magnetic measurements, one can evaluate the growth of RE in time using: $\frac{d}{dt} \int j_{RE} dS = -\frac{dI_{pl}}{dt}$.

Figure 7 summarizes the dependence of RE current conversion rate versus CQ rate values at disruptions. One can see that CQ rates in smaller devices should be approximately 10 times higher than in large tokamaks in order to cause comparable RE generation at disruptions. Simple calculation using the CQ data from figures 6(b) and 7 shows that CQ rate evolution from COMPASS to JET depends not only on I_{pl}, B_0, n_e, T_e, etc, but also on the value of plasma total inductance determined by the major and minor plasma radii of the devices: $L_p = \mu_0 \cdot R_0 \cdot (\ln(8R_0/a_p)–2)$. In the same time, measured CQ rates allowed to deduce the ranges of average post-disruption plasma temperatures: $T_e \leqslant 7$ eV in COMPASS, $T_e \leqslant 10$ eV in ASDEX-Upgrade and $T_e \leqslant 20$ eV in JET. Therefore, the devices with larger geometrical sizes and higher plasma operational parameters, i.e. large tokamaks [2], provide wider limits of the spatial and temporal evolutions of plasma parameters during disruptions, thus extending the parameter space for RE generation.

Small and medium sized tokamaks revealed characteristics of RE in MGI disruptions similar to those in JET-C and JET-ILW. However, significant differences in RE parameters have been found also. In particular, the RE experiments in COMPASS (with carbon limiter) have demonstrated obvious non-increasing trend in generated RE currents versus plasma current time derivatives (figure 8(*a*)). This result is quite different from the data collected in JET-C, where the stable increasing trend of generated RE current versus plasma current time derivative was found [11]. Note that this JET-C trend is based on the data obtained in spontaneous disruptions and those triggered by slow gas puff. In contrast to this data from JET-C, MGI experiments in JET-ILW did not demonstrate such an obvious trend [33].

The change of plasma current direction in COMPASS also resulted in certain differences in runaway generation parameters. This difference could be linked to the change of the helicity direction at unchanged directions of the plasma particles drifts due to grad-B. It is expected to extend the data presented in figure 8(*b*), because, the availability of a small number of this data may be misleading.

Despite the observed similarity in the sequence of processes during disruptions, a strong difference between the RE plateau current average densities in JET-ILW and ASDEX-Upgrade has been found. The pre-disruptive average densities of plasma currents have been evaluated: $\langle j_{pl} \rangle \approx 0.5$ MA m^{-2}—in JET and $\langle j_{pl} \rangle \approx 0.8$ MA m^{-2}—in ASDEX-Upgrade (figure 9). After disruptions the average current densities of RE plateaux in JET remained close to pre-disruption values. Sometimes the increase of average RE current density was observed achieving almost 2 times larger values at the time of plateau termination. Meanwhile, during ASDEX-Upgrade disruptions the runaway acceleration provided the average density of RE plateaux about 2–3 times lower relatively to pre-disruptive values and there were no indications for similar to JET increase of the RE current density during plateaux. This result could be explained by the fact that characteristic e-folding time of plasma current decay in JET is $8 \leqslant t_{CQ} \leqslant 12$ ms, which is significantly larger than in ASDEX-Upgrade ($t_{CQ} \approx 2$–3 ms). Therefore, sustained for a longer

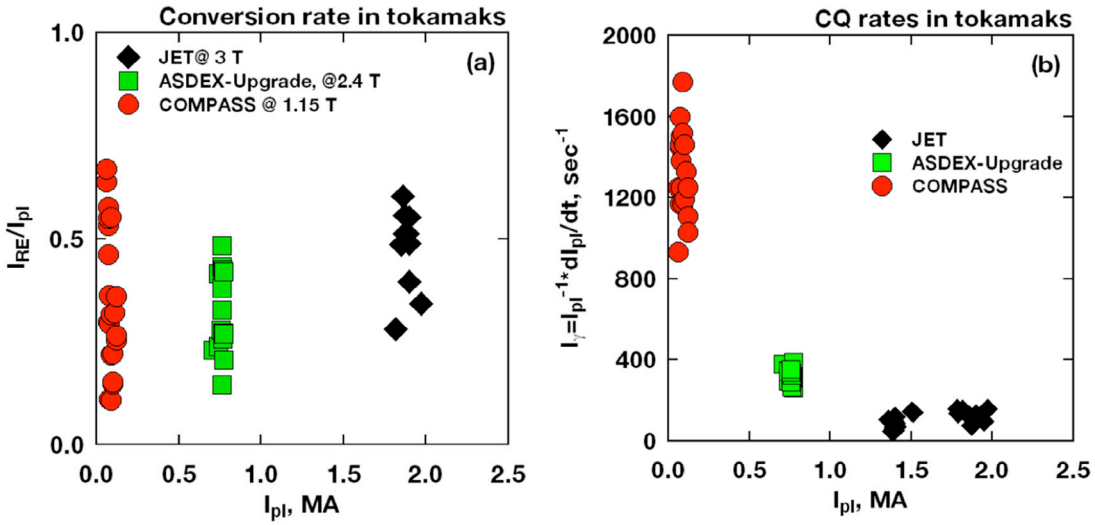

Figure 6. Conversion of plasma currents into RE currents—chart (*a*), and CQ rates in disruptions with RE generation—chart (*b*) in small medium-sized and large tokamaks.

time the runaway process in JET provides accumulation of higher RE density. With the increase of RE fraction in total current during CQ the generation process is self-limited by the decrease of electric field. At the sufficient decrease of electric fields the generation of new REs is ceased and the remaining plateau current is carried by RE.

The second possible reason for the observed difference between parameters of RE plateaux in JET and ASDEX-Upgrade is the difference between the values of lost plasma currents due to the current peeling effect. This effect inevitably occurs during fast inward motion of the plasma on CQ and it should result in higher electric fields due to the additional loss of the corresponding magnetic flux [39].

Yet another reason for observed difference could be the substantially shorter gas travelling distance from in-vessel valve to the plasma after MGI in ASDEX-Upgrade. As a result, the faster gas penetration, better its assimilation and more effective RE dissipation could be achieved. Similarly to the results from the D-IIID tokamak [28], the ASDEX-Upgrade experiments have shown dissipative effects of the second MGI of Ar/Ne on RE beams for both, far and close located injection valves [30].

In contrast to D-IIID [28] and ASDEX-Upgrade [30] the dissipative effect of secondary MGI on already accelerated RE beam was not achieved in JET [12, 13]. These JET experiments have demonstrated the presence of low temperature but dense enough post-disruption background plasma ($\bar{n}_e \leqslant 10^{20}$ m^{-3}), which fills almost all vacuum volume comprising the space of open magnetic field lines and nested magnetic surfaces formed by RE beam current [12, 13]. Interacting with background hydrogen neutrals and impurity ions relativistic RE, both, well confined and already drifted out, can generate secondary (not runaway) electrons [40–43]. The ionization cross-section of hydrogen by relativistic electron is described in [40]. Subsequently, for an ion X_i with ionization potential I_{X_i} and having N_{X_i} outer shell electrons the formula for cross-section ionization by relativistic electron with energy characterized by Lorentz factor γ_0 was derived in the form [41, 42] given below:

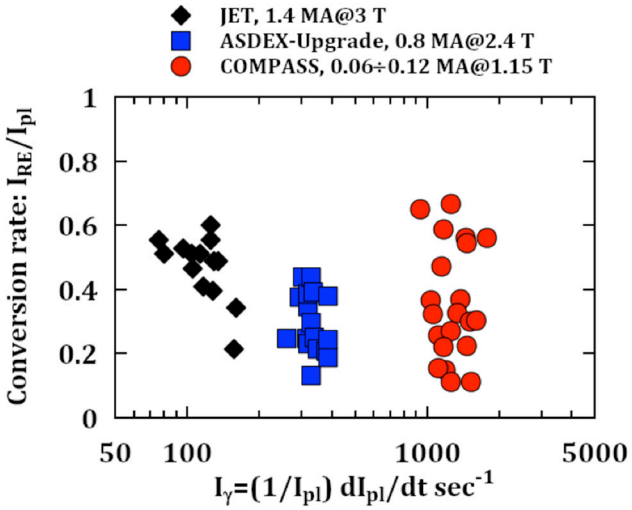

Figure 7. Dependence of conversion rate of plasma resistive currents into RE currents versus CQ rates at disruptions in tokamaks (values of disrupted currents are given in header).

$$\sigma_{X_i} = 7.24 \cdot 10^{-20} \frac{N_{X_i}}{I_{X_i}} \cdot \frac{\gamma_0^2}{\gamma_0^2 - 1} \left(15.85 - \ln(I_{X_i}) + 2\ln(\gamma_0)\right). \quad (1)$$

In [42, 43] it was pointed out that relativistic electron ionization could generate low temperature electrons with mean energy ~40 eV. Analysis of the spectroscopy data measured during the runaway plateaux in JET indicates the presence of argon lines with wavelengths corresponding to 3- and 4-times ionized Ar. This data well corresponds to the statement above, since to achieve observed Ar ionization stages the background plasma should have significant electron temperature $10\,\text{eV} \leqslant T_e \leqslant 20\,\text{eV}$ [44]. Therefore, the ionization of background gas by RE serves as a source for plasma cloud, which surrounds the RE beam [12, 13]. It is obvious, that such plasma will have a screening effect on the penetration of the injected gas [45] to the location of RE beam thus decreasing the effect of the second MGI.

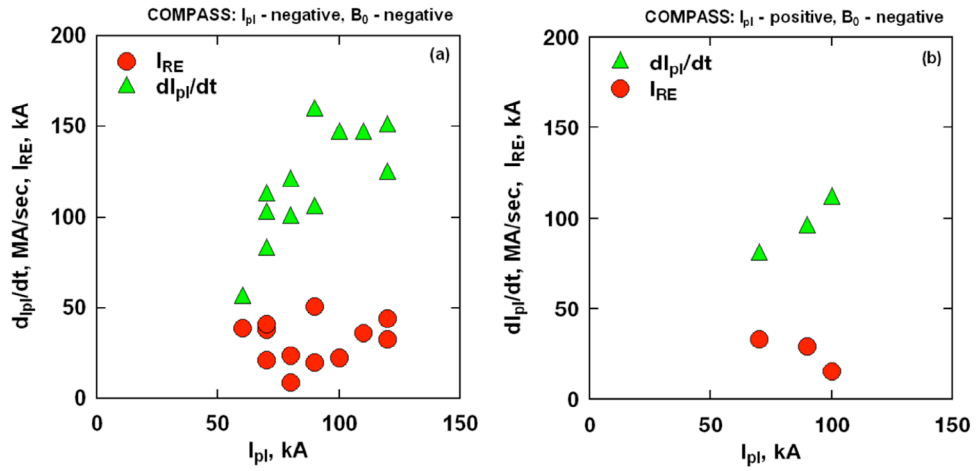

Figure 8. A study of RE generation at inversion of plasma current direction in COMPASS disruptions: (*a*)—plasma currents and B_0 are in co-direction; (*b*)—plasma currents and B_0 are in counter-direction.

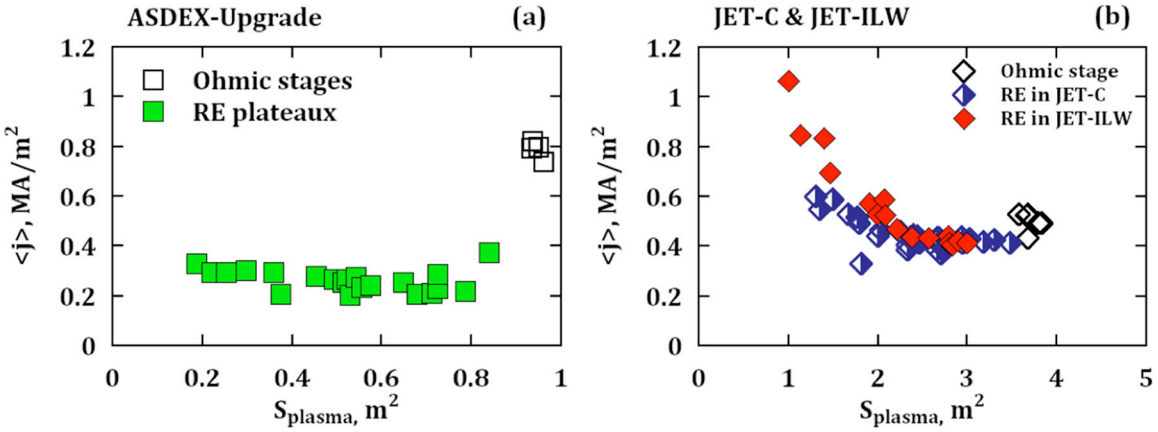

Figure 9. Comparison of average RE current plateaux densities in ASDEX-Upgrade (*a*) and in RE plateaux in JET-C and in JET-ILW (*b*) generated during disruptions triggered by MGI.

4. RE in stationary discharges in TCV, COMPASS and JET

4.1. Runaway critical energies and runaway critical electric fields in tokamaks

Transient nature of disruptions does not allow reliable measurements of plasma parameters evolution. Modelling of RE generation at disruptions is still very complicated task also, since it requires an inclusion of many parameters, which are strongly varied during disruptions. Therefore, a scenario of RE generation in stationary discharges in tokamaks constitutes a subject of special attention due to possibility to measure reliably plasma parameters during onset, growth and loss of relativistic RE [34]. This steady-state scenario with low plasma density was used in the second group of experiments in COMPASS and TCV. Obtained data on RE generation dynamics was compared to the data measured during RE stationary phase of the JET discharge JPN #86078 [35].

The baseline scenario for RE studies in TCV is: L-mode, inner wall limited Ohmic discharges ($R_0 = 0.89$ m, $a_{pl} = 0.25$ m) at $B_0 = 1.43$ T, plasma currents $I_{pl} \leqslant 200$ kA and average plasma density $\langle n_e \rangle \leqslant 3{\cdot}10^{19}$ m^{-3}. Conditions for measurable RE generation during flattop were achieved by controlled plasma density ramp-down (figure 10).

RE in COMPASS are normally produced during the current ramp-up phase providing the measurable seed RE population detected using HXR diagnostics. The baseline scenario for RE studies is: $B_0 = 1.15$ T, 90 kA $\leqslant I_{pl} \leqslant$ 150 kA, $\langle n_e \rangle \leqslant 3 \cdot 10^{19}$ m^{-3}, Ohmic inner wall limited discharge in L-mode. Using different fuelling scenarios the RE populations could be generated (figure 11) allowing studies of MHD effects on RE confinement [31].

Similarly to the JET data, plasma parameters in COMPASS and TCV have been numerically processed in order to minimize the effect of the data large scattering (filtering noise, etc) onto results of numerical evaluation of runaway dynamics. All measured parameters were used in simulation of runaway generation in radially averaged model with the aid of iterative method [20]. In this modelling the value of effective ion charge (Z_{eff}) was used as iterative parameter and calculated using the equation of plasma electro-conductivity on the basis of measured plasma current, loop voltage (V_{loop}), electron temperature (T_e) and density $\langle n_e \rangle$.

Analysis of stationary RE discharges in COMPASS, TCV and JET [35] has shown that the primary (Dreicer) process

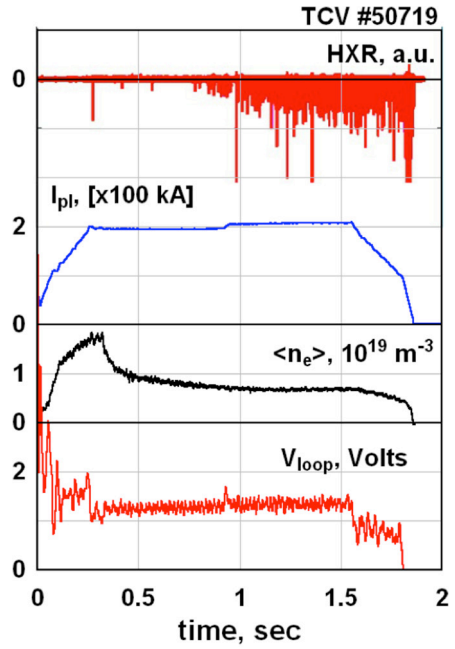

Figure 10. RE generation scenario in stationary discharge in TCV.

is dominating in these series of experiments. In low-density stages the mean velocities of plasma current increased up to $u_0 \equiv \frac{<j_{pl}>}{e<n_e>} \cong 10^6$ m s^{-1} in COMPASS, $\cong 4.0 \cdot 10^6$ m s^{-1} in TCV and $\cong 3 \cdot 10^6$ m s^{-1} in JET. One can see that achieved asymmetry of electron distribution function (EDF) at corresponding streaming parameter $\xi^* \equiv \frac{u_0}{v_{T_e}} \cong 0.1$ should result in increase of the number of electrons (up to 10%) moving in a velocity space close to and above the critical runaway velocity [46]

$$v_{CR} = \sqrt{\frac{e^3 n_e \ln\Lambda\ (2 + Z_{eff})}{4\pi\varepsilon_0^2 m_e E_0}}. \tag{2}$$

This velocity is determined by the balancing between the electron acceleration in external electric fields (E_0) and the dissipative drag, i.e. when electrons achieve $v_e > v_{CR}$, they become runaway. Corresponding critical threshold in kinetic energy for runaway process is

$$W_{CR} \equiv \frac{m_e v_{CR}^2}{2} = \frac{e^3 n_e \ln\Lambda\ (2 + Z_{eff})}{8\pi\varepsilon_0^2 E_0}. \tag{3}$$

This threshold is only a parameter, which is valid for characterization of both main mechanisms responsible for RE generation in stationary discharges—primary (Dreicer) and secondary avalanching [17–19]. In COMPASS, TCV and JET the critical energy (W_{CR}) varied between ≈10–40 keV and ≈100–120 keV depending on electric fields and other plasma parameters. In terms of electric fields one can formulate that the runaway generation will develop if applied electric field E_0 will exceed a certain critical value (E_{CR}) determined by the balancing between energy gain and dissipation. For electron populations with thermal velocities $v_{T_e} = \sqrt{kT_e/2m_e} \ll c$ (non-relativistic energies), the runaway critical field is

$$E_{CR} \equiv E_{DR} = \frac{e^3 n_e \ln\Lambda\ (2 + Z_{eff})}{4\pi\varepsilon_0^2 m_e v_{T_e}^2}. \tag{4}$$

This field (E_{DR}) characterizes the primary (Dreicer) runaway generation process. If $E_0 \geqslant E_{DR}$ all plasma thermal electrons will runaway. For typical plasma parameters in tokamaks with EDF close to Maxwell distribution $E_0 \ll E_{DR}$, so that only an exponentially small population of the electrons from the tail of EDF will experience collisionless acceleration with generation rate [47]:

$$\lambda_R = C(Z_{eff}) \cdot n_e \nu_{ee} \varepsilon^{-\frac{3(Z_{eff}+1)}{16}} \cdot \exp\left(-\frac{0.25}{\varepsilon} - \sqrt{\frac{Z_{eff}+1}{\varepsilon}}\right). \tag{5}$$

Here ν_{ee} is collision frequency and $\varepsilon = E_0/E_{DR}$. Primary rate is strongly depending on plasma density and temperature (T_e). Large asymmetry of EDF provides an additional electron flux into runaway regimes.

The RE generation dynamics on the basis of measured plasma parameters for all experiments was modelled using an equation for the radially averaged RE density (n_{RE}) evolution

$$\frac{dn_{RE}}{dt} = \lambda_R + \frac{n_{RE}}{t_0} - \frac{n_{RE}}{\tau_{conf}}. \tag{6}$$

A perfect RE confinement is assumed, i.e. infinite runaway electron confinement time: $\tau_{conf} = \infty$, because, during the times of interest in these experiments an attainable maximum of RE kinetic energy is much higher than in fact possible RE energy increase. Since the RE generation occurs on steady state of low-density discharges in all tokamaks, the dominating source of RE is the Dreicer mechanism. In fact, during transient processes, like disruptions, which are resulting in fast plasma cooling the hot tail generation could be the dominating mechanism to generate seed RE [21–23, 48]. In our studies the primary generation provides the seed RE population (the first term in equation (6)) for further possible development of runaway process due to avalanching of secondary RE [17–19].

The evolution of RE density due to secondary avalanching is characterized by the second term in equation (6), where t_0 is characteristic avalanching time. Corresponding growth rate of secondary avalanching is $\gamma_{AV} = 1/t_0$. The avalanching time was proposed on the basis of the analysis of the integral of close collisions [18] in the following form:

$$t_0 = \frac{\sqrt{12}\ln\Lambda\ m_e c\ (2 + Z_{eff})}{9eE_0}. \tag{7}$$

This parameter is inferred in assumption that there are seed RE with high energies (>1 MeV) and accelerating electric field is much higher than critical one (tens V m^{-1}), as it usually observed during disruptions [18, 49, 50]. In more general case, the parameter t_0 depends not only on E_0, but also on the critical field determined by drag force acting on relativistic electrons. The critical field for relativistic electrons was derived in [47] as: $E_R = \frac{e^3 n_e \ln\Lambda}{4\pi\varepsilon_0^2 m_e c^2}$. It was shown that relativistic

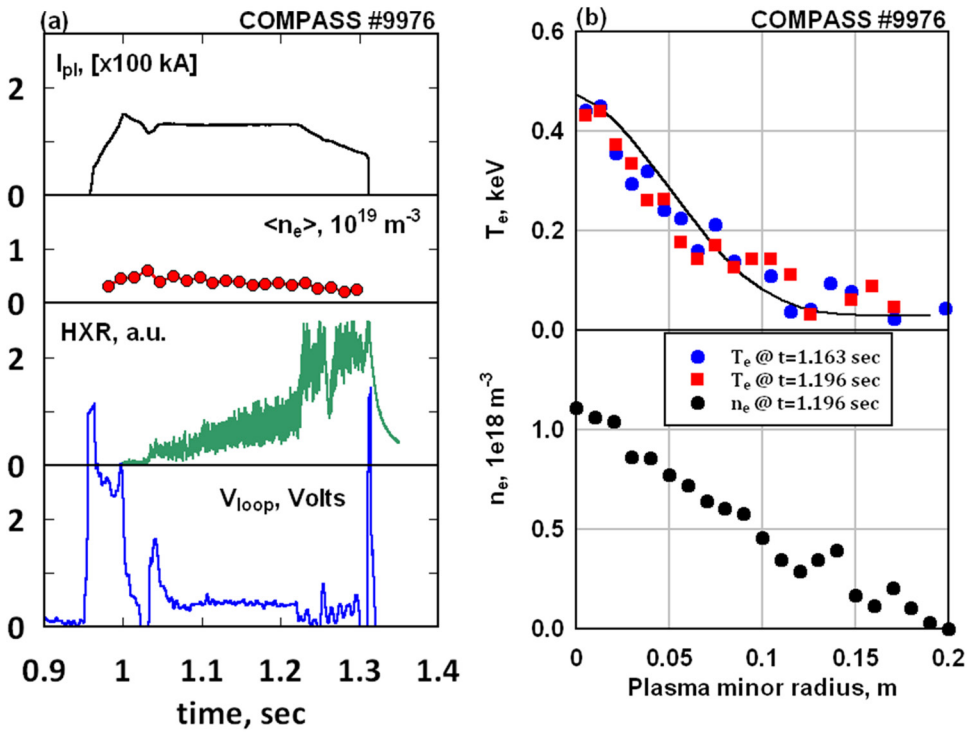

Figure 11. Chart (*a*)—evolutions of plasma parameters in RE generating discharge in COMPASS; chart (*b*)—examples of electron temperature and density profiles measured by Thomson scattering diagnostics during RE generating stage.

effects as well as effect of plasma impurity ions ($Z_{\rm eff}>1$) significantly modify the dynamics of runaway process. The critical field derived in [47] subsequently was proposed as a threshold field ($E_{\rm CR\_AV}$) for avalanching process [19, 24, 48], etc, so that $E_{\rm CR\_AV}=E_{\rm R}$. In a majority of recent studies the avalanching time t_0 is calculated using the interpolation formula [19]

$$t_0=\frac{4\pi\varepsilon_0^2m_{\rm e}^2c^3}{e^4n_{\rm e}(\alpha-1)}\sqrt{\frac{3}{\pi\varphi}(Z_{\rm eff}+5)}\cdot\sqrt{\frac{\alpha-1}{\alpha}+\frac{4\pi\cdot(Z_{\rm eff}+1)^2}{3\varphi\cdot(Z_{\rm eff}+5)(\alpha^2+\frac{4}{\varphi^2}-1)}}. \quad (8)$$

Here, $\varphi=\left(1+1.46\sqrt{r/R_0}+1.72\cdot r/R_0\right)^{-1}$, $\alpha=E_0/E_{\rm CR\_AV}$. This formula (8) was derived on the basis of analytical solution of the bounce-averaged relativistic Fokker-Planck equation in different limits [19, 48]: for $E_0\gg E_{\rm R}$ when pitch-angle scattering is neglected and when pitch-angle scattering is dominant; and near critical field ($E_0\geqslant E_{\rm R}$).

In fact, the growth rates calculated according to both formulas, (7) and (8) [18, 19] at the presence of relativistic RE and very large electric fields ($E_0\gg E_{\rm CR\_AV}$) that usually measured during disruptions are very close. Numerical evaluation of RE generation at disruptions in frames of both approaches confirmed their validity yielding the values of RE currents in adequate agreement to the experimental ones [10, 11]. In opposite case, the RE growth rate should vanish if $E_0\leqslant E_{\rm CR\_AV}$, and, therefore, below $E_{\rm CR\_AV}$ (or $E_{\rm R}$) no runaway generation will occur ([34] and references cited therein). However, in experiments the condition $E_0>E_{\rm CR\_AV}$, which is considered to be sufficient for generation/avalanching of RE [34], does not signify that these processes should inevitably occur. Low-density stationary discharges in COMPASS,

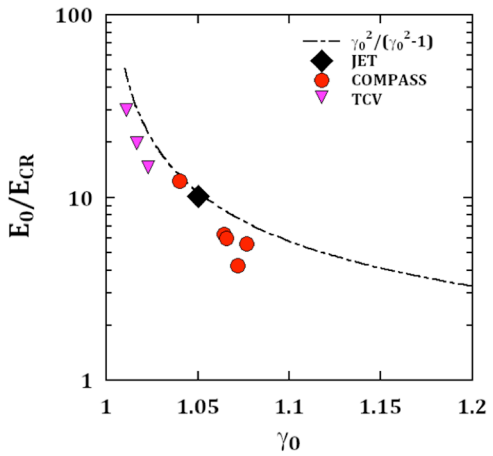

Figure 12. Critical electric fields for different critical energies in RE generating discharges in tokamaks: data of several discharges from COMPASS and TCV and one JET pulse is presented.

TCV and JET [35] are characterized by enhanced generation of primary RE at very low critical energies. Critical field for this process is significantly higher than $E_{\rm R}$. In particular, for energies, which are substantially lower than relativistic case (which is ~mc^2), the drag force acting on accelerated electrons is significantly higher than for relativistic RE and corresponding critical field is

$$E_{\rm CR}=\frac{e^3n_{\rm e}\ln\Lambda\,(2+Z_{\rm eff})}{4\pi\varepsilon_0^2m_{\rm e}c^2}\cdot\frac{\gamma_0^2}{\gamma_0^2-1}. \quad (9)$$

One can see that the critical field will be much higher than asymptotic relativistic value ($E_{\rm R}$) at critical energies $\gamma_0\approx1.05$–1.1 ($W_{\rm CR}$ is of the order of tens keV). The data on

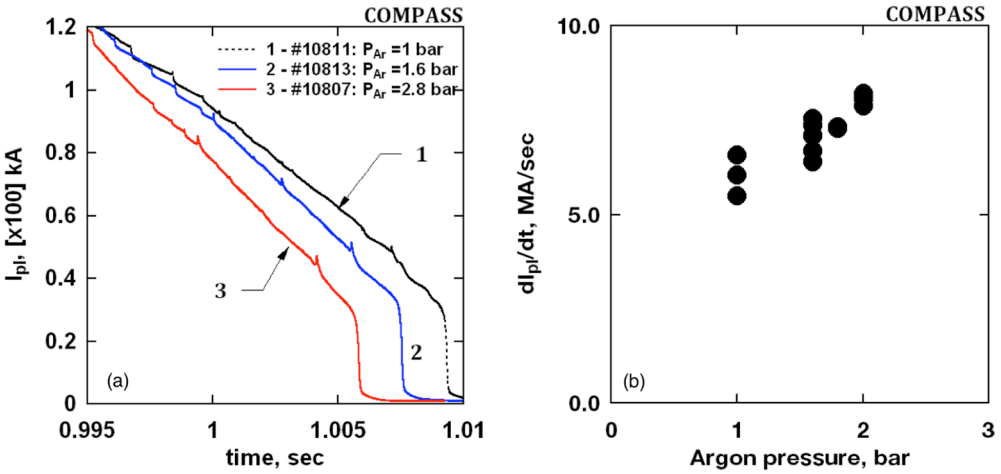

Figure 13. MGI into RE generating discharges in COMPASS: chart (*a*)—scenario for slow dissipation of RE beams using Ar injection; chart (*b*)—summary on dissipative effect of Ar injection on RE populations.

critical fields inferred from the parameters of runaway generation dynamics in COMPASS, TCV and JET [35] discharges fits well to this dependence (figure 12).

4.2. MGIs into stationary RE beams in tokamaks

Close distance collisions are less frequent than usual long-distance Coulomb collisions by a factor $8 * \ln\Lambda$, here $\ln\Lambda$ is the Coulomb logarithm. Therefore, at very low background electron densities the frequency of close distance collisions does not enable the avalanching despite the presence of high energy RE: $\gamma_{AV} \leqslant 1$ according to formula (8). Condition for avalanching requires the presence of both, substantially higher plasma densities and seed RE electrons with very high energies. In [49] the RE avalanching dynamics was studied using numerical modelling depending on background plasma density. The increasing trend in avalanching of secondary RE with the increase of plasma density was demonstrated.

The RE avalanching has been examined in RE experiments on TEXTOR [50, 51]. Ne puffs into discharges with small RE fractions were used to study the control of runaway process by changing Z_{eff}. In [50] authors reported that variation of Z_{eff} was $1.5 \leqslant Z_{eff} \leqslant 2$. In [51] authors claimed that the increase of Z_{eff} was varied in limits $0.7 \pm 0.2 \leqslant \Delta Z_{eff} \leqslant 4 \pm 1$. After the Ne puff the signals of HXR, electron cyclotron emission (ECE), photo-neutrons and data from infrared (IR) diagnostic indicated significant changes of RE parameters, which have been linked to onset of avalanching. However, the changes in neither Z_{eff} nor plasma density did not result in generation of significant populations of secondary RE due to insignificant change of the avalanching growth rate $\gamma_{AV} \sim 1$ [51].

Recent experiments with massive injections of Ne and Ar into stationary discharges with large RE populations have been carried out in COMPASS and TCV in order to mock-up the RE suppression experiments carried out in JET-ILW [12, 13]. In JET the first injection of Ar/Ne from DMV was used as usual trigger for disruptions with RE generation and MGI from the second DMV was applied during RE plateaux to study the dissipative effects of

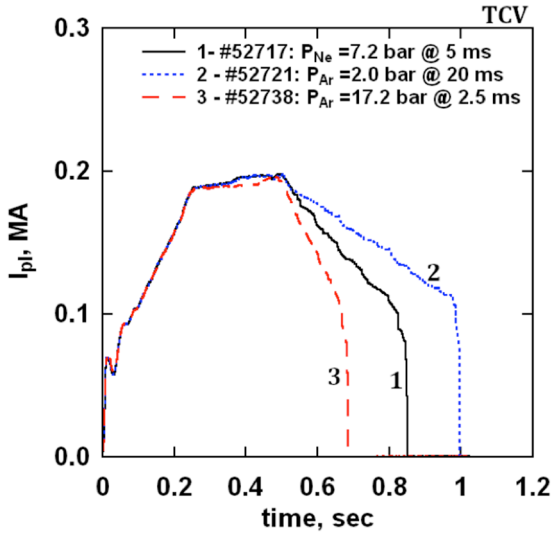

Figure 14. Scenario for study of interaction of RE populations with MGI of different impure gases into RE generating discharges in TCV.

impure gases on runaways [12, 13, 33]. Impurity injections into RE dominating discharges in TCV and COMPASS had purpose to investigate an interaction of RE beams with large quantities of injected impure gases and to distinguish dissipative effects.

The first massive injections of Ar in discharges with RE populations in COMPASS allowed establishing the regimes with relatively slow termination of the currents with RE fractions (figure 13(*a*)). Plasma current time derivative in these discharges (dI_{pl}/dt) has been used as a parameter for assessment of dissipative effect of Ar injections. This parameter has been varied between 1 and 10 $MA \cdot s^{-1}$ and increased with the increase of injected Ar quantity (figure 13(*b*)).

A study of RE dynamics depending on amount and type of injected gas was carried out in TCV using injections of Ne and Ar into stationary stage of RE discharges (figure 14). In was found that impurity with higher Z (for example, Ar in comparison to Ne) resulted in faster RE current termination indicating stronger dissipative effect on runaways. Similarly

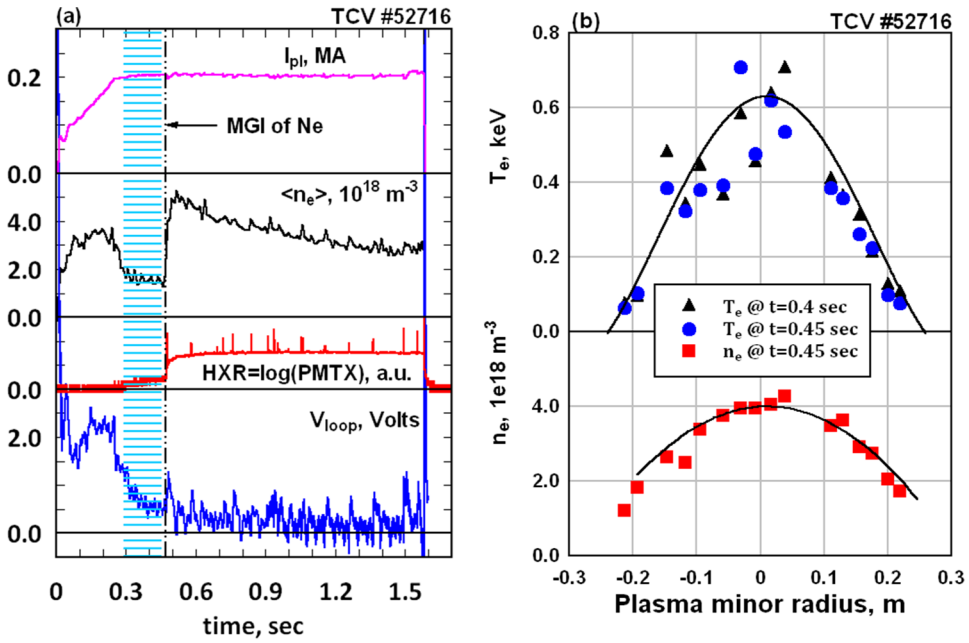

Figure 15. Injection of Ne during RE generating stage in the discharge #52716; RE generating stage is marked in light blue in left chart (*a*) and MGI time is indicated by vertical dotted line; right chart (*b*)—profiles of electron temperatures and density measured by Thomson scattering diagnostics during RE generating stage in times before MGI.

to COMPASS, the increase of injected Ar quantity has demonstrated more efficient RE current dissipation.

In experiments on interaction of RE populations with Ar/Ne injected in TCV a new evolution of RE stationary discharges without slow termination and disruptions has been discovered. Subsequent analysis of the measured plasma parameters suggests the link of observed phenomena to the process of secondary RE avalanching in TCV. A new data on the avalanching of secondary RE was collected and studied.

Figure 15 (chart (*a*)) presents temporal evolutions of the main plasma parameters in TCV pulse #52716, which entered into RE generation regime following the programmed plasma density ramp-down. Plasma density decrease from $t \approx 0.35$ s to $t = 0.45$ s, subsequent decrease of $\langle V_{\rm loop}\rangle$ from ≈0.85 V to ≈0.56 V and appearance of HXR (PMTX) signal are appropriate indications of RE generation (this stage is marked by light blue colour). Quantification of RE generation process has been carried out in 0D-model (radially averaged) using the same approach as in [11, 20]. The measurements of electron temperature and density using Thomson scattering diagnostic ($T_e(r)$, $n_e(r)$, see figure 15, chart (*b*)) and the measured macroscopic plasma parameters $V_{\rm loop}$, $\overline{n_e}$ and $I_{\rm pl}$ have been numerically processed to benchmark the conformity of all experimental data. For this the equation for plasma electroconductivity with inclusion of RE generation was solved self-consistently by iterations using $Z_{\rm eff}$ as iterative parameter [20].

The Dreicer generation is the main source for RE in the first several hundreds milliseconds of the stationary low-density discharges in TCV. Numerically processed experimental data has been used to calculate the primary (Dreicer) generation till to $t = 0.45$ s (figure 15, left chart). It is found that RE with average density up to $\overline{n_{\rm RE}} \leqslant (5\text{–}6) \cdot 10^{15}$ m^{-3} could be generated. This density corresponds to the average RE current density ~250 kA m^{-2}, so that, the RE component in a total plasma current does not exceed ≈40–50 kA. The critical runaway energy in this stage was ≈50 keV. Using the measured loop voltage and taking into account that electric field in the plasma centre is lower ($T_e(0) \approx 700$ eV) one can assess the maximum energy of RE, which reaches up to ⩽1–1.5 MeV. This result is supported by measurement of very small HXR (PMTX) signal. Calculated from the measured plasma parameters an avalanching growth of the secondary RE during this stage was absent or negligibly small ($\gamma_{\rm AV} \leqslant 1$) due to the low density and frequency of close distance collisions.

Massive Ne injection at $t = 0.47$ s significantly changed the evolution of plasma and RE parameters. However, neither discharge disruption, nor slow discharge termination due to fast plasma cooling has been occurred. Plasma density increased up to ~$(5\text{–}6) \cdot 10^{18}$ m^{-3} during less than 10 ms. During the same time, the almost complete thermal collapse occurred resulting in decrease of electron temperature from $\overline{T_e} \approx 300$ eV to $\overline{T_e} \leqslant 50$ eV. Simultaneously to density increase and $\overline{T_e}$ collapse a large increase of stationary HXR emission (PMTX signal) was measured (figure 15). Together with the increase of stationary HXR emission (PMTX signal) the intense HXR bursts were measured during whole remaining discharge stage. Their magnitude reached up to ~10 times higher values than stationary signal level.

During T_e collapse the fast increase of $V_{\rm loop}$ up to ≈1.2 V was measured. Soon after observed increase (in ≈ 10–15 ms), $V_{\rm loop}$ decreased to the value even lower than pre-injection one: $\langle V_{\rm loop\_filtered}\rangle \approx 0.25$ V despite the high plasma resistance. Time resolved analysis of the plasma and RE parameters on this stage has shown that electric field in plasma during transition could reach more than 10 times higher value in comparison to that measured on plasma surface. Therefore, a combination of such significant increases of plasma density and E_0 resulted in corresponding increase of avalanching

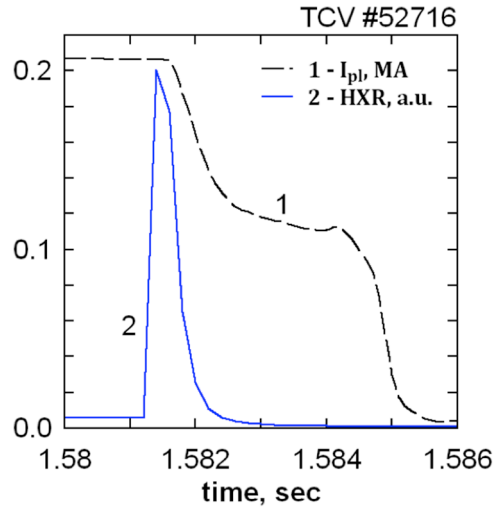

Figure 16. Termination of TCV discharge #52716: HXR signal is saturated due to intense HXR emission burst following the loss of RE population.

growth rate. For certain time interval the avalanche growth rate was even higher than 100, thus providing the generation of large RE population. The duration of discharge transition into low voltage phase (~10 ms), the ranges of $\overline{T_e}$ decrease and density increase, and the presence of already generated primary RE rule out possible significant contribution to RE generation due to hot-tail mechanism [22, 23, 48].

After the transition, the V_{loop} signal quickly decreased indicating the self-limiting of avalanching process. Evaluation of the RE density dynamics (equation (6)) with calculated avalanching growth rate demonstrated that after transition RE could carry up to 150 kA in a total plasma current in this discharge. This value corresponds to the average RE current density ~800 kA m^{-2}. The RE current fraction corresponding to calculated RE density is consistent with the results of assessment of the RE current fraction from the analysis of the measured loop voltage evolution: $\sigma_{pl}(t)E_0(t) = j_{OH}(t) - j_{RE}(t)$, where $E_0 = V_{loop}/2\pi R_0$ and $\sigma_{pl}(t)$ is a plasma conductivity.

This discharge lasted till to $t = 1.581$ s when it was terminated by disruptive-like event following the negative loop voltage spike. During this termination an intense burst of HXR emission was detected. In the same time a loss of approximately of one half of the total plasma current was measured (figure 16). A loss of the remaining current fraction after $t = 1.584$ s did not indicate any evidence (HXR, etc) of the presence of any energetic electron population in residual current. Analysis of plasma parameters during decay stage of #52716 yielded slightly lower RE current fraction ($I_{RE} \approx$ 90–100 kA). Therefore, despite the uncertainties caused by measurements, numerical data processing and limitations of 0D-model, the values of RE current calculated in stationary discharge are in acceptable conformity to the value of RE fraction deduced from the measured experimental parameters during discharge termination.

4.3. Analysis of instability events in RE dominating discharges in TCV

The relaxation events and RE losses were detected from the time of discharge transition into low-voltage phase in many TCV pulses (for example, #52711, #52712, #52716, etc). In particular, from this time the abrupt intense bursts of HXR coinciding with characteristic positive/negative spikes in V_{loop} signal and small decrease step-like relaxations in the plasma current signal I_{pl}, etc were measured (figure 15). Detected relaxations in TCV are very similar to those observed in discharges with large populations of RE in early tokamak experiments [52, 53] and in recent studies [16, 20, 54, 55].

Usually relaxation processes in plasmas with large RE populations are addressed to the excitation of kinetic instability, which is driven by RE due to anomalous Doppler effect [56, 57]. These studies investigated a stability of non-relativistic RE distributions relatively to the anomalous Doppler resonance considering different threshold conditions for this kinetic instability. The instability threshold proposed in [56]: $v_{beam} > 3v_{CR} \cdot (\omega_{ce}/\omega_{pe})^{3/2}$ is often applied in analysis of instability parameters for non-relativistic or, sometimes, weakly relativistic RE distributions in medium and small tokamaks during last couple decades [16, 20, 54, 55]. Analysis of many RE discharges with instability events revealed a satisfactory agreement of their parameters to this threshold [20, 54, 55].

The critical runaway energy in the low-density TCV discharges before the transition was ≈50 keV. Though the critical runaway velocity reached mildly relativistic values after the transition, nevertheless, events related to the instability were observed. According to [57] the instability should occur at higher RE beam velocities than predicted in [56], thus appearing to be out of frames of non-relativistic model. Therefore, the model for kinetic RE instability should include the relativistic effects.

Significant efforts have been done recently in the development of modelling tools for study of RE beam stability with inclusion of relativistic effects in a view of importance of RE generation problem in ITER [58]. In particular, the kinetic instability thresholds for different RE energies calculated using the numerical tool developed in [58] fit well to empirically determined criterion for the RE driven instability in different tokamaks [53]. This quite simple condition expressed in terms of averaged plasma parameters $j_{RE}/(1.4 \cdot n_e) \geqslant 1$, where j_{RE}—in MA m^{-2} and n_e—in 10^{19} m^{-3}, has been used to examine the parameters of RE dominating discharge #52716 in TCV. Two data points have been analysed—before Ne injection and after, when discharge #52716 entered into low-voltage phase. One can see, that data point corresponding to the stage before MGI ($t \leqslant 0.45$ s) with calculated average RE current density ~0.25 MA m^{-2} and measured average plasma density ≈(2–2.5) · 10^{18} m^{-3} is located well below the empirical criterion and modelled instability thresholds (see figure 4

in [58]). Meanwhile, after transition the evaluated RE current density becomes $\langle j_{RE} \rangle \approx 0.8$ MA m^{-2}. And even at observed increase of plasma density till to $\approx 5 \cdot 10^{18}$ m^{-3} this point satisfies well to the criterion when instability occurs. In [58] it was confirmed that in experiments of [52, 53] the magnetized plasma wave was the main unstable mode.

The analysis of discharge #52716 in TCV has demonstrated the conformity of plasma parameters in this RE dominating discharge to the threshold parameters for the kinetic instability driven by RE given in [56–58]. Moreover, these parameters satisfy to conditions of empirical threshold for RE instability. However, the question about the most unstable mode for observed instability in TCV is still open, since the instability has been detected in sufficiently wide range of parameters: $10\,\text{eV} \leqslant \overline{T_e} \leqslant 60\,\text{eV}$ and $n_e \leqslant (4\text{–}6) \cdot 10^{18}$ m^{-3}, that substantially complicates the mode identification [56–58].

A detailed analysis of the data on kinetic instability driven by RE obtained in recent experiments in the TCV tokamak will be a subject of future separate study to provide more information on parameters of instability for numerical simulations and to clarify possible processes capable to destabilize the disruption generated RE beams in tokamaks.

5. Summary

(1) The first series of experiments on RE, disruption generated and in stationary discharges, have been carried out in small and medium-sized tokamaks—COMPASS, TCV and ASDEX-Upgrade, in support to RE studies in the large tokamak—JET with ITER-like wall. The most reliable disruption scenarios with RE generation have been designed for future RE experiments.

(2) Disruption scenario for deuterium, hydrogen and helium plasmas in ASDEX-Upgrade has demonstrated the possibility to generate RE plateaux with currents up to 0.4 MA, duration up to 0.4 s and RE energies up to 10 MeV that is comparable to RE parameters in JET disruptions. Disruption scenario with MGI of Ar in COMPASS resulted in RE current plateaux with values up to 60 kA and duration up to 20 ms. These scenarios are foreseen for future studies of the dissipative effects of MGI on RE beams to provide the experimental data supporting the advances in the physics of runaways and the development of disruption mitigation system in ITER.

(3) New data on RE generated during disruptions in COMPASS and ASDEX-Upgrade was collected and added to the JET database. These results from small and medium-sized tokamaks have demonstrated their conformity to the RE data obtained in JET. It was also shown, that tokamaks with bigger geometrical sizes provide the wider limits for spatial and temporal variation of plasma parameters during disruptions, thus extending the parameter space for RE generation.

(4) Generation of RE beams with the measured currents about of tens/hundreds kA at magnetic fields $B_0 = 1\text{–}1.2$ T in JET-ILW and COMPASS evidently indicates about the absence of the so-called 'threshold' for RE generation on toroidal magnetic field value.

(5) Parameters of RE generation in stationary discharges including runaway critical fields and energies have been evaluated for JET, COMPASS and TCV. In all low-density stationary discharges the primary (Dreicer) mechanism was the main source for RE generation according to theory, since the low frequencies of close distance collisions and low critical runaway energies constrained the avalanching growth of secondary RE.

(6) The evaluation of runaway critical electric field for stationary low density discharges in JET, TCV and COMPASS have demonstrated an expected from the theory the dependence of critical field on electron energies in sub-relativistic energy range. This critical field exceeds the relativistic runaway critical field by a factor of 4-30 in different discharges and devices.

(7) Secondary RE avalanching was identified and quantified for the first time in the TCV tokamak in RE generating discharges after massive Ne injection. Simulations of the primary RE generation and secondary avalanching dynamics in stationary discharges has demonstrated that RE current fraction created via avalanching could achieve up to 70–75% of the total plasma current in TCV. This result is in adequate accordance to the value of RE current fraction deduced from the measured parameters during discharge termination stage.

(8) Relaxations of plasma parameters have been detected in RE discharges in TCV. These relaxations are reminiscent the phenomena associated to the kinetic instability driven by RE. Accomplished analysis of the experimental data has clarified that observed relaxations should be associated to the excitation of the kinetic instability driven by relativistic RE. Macroscopic parameters of RE dominating discharges in TCV before and after onset of the instability fit well to the empirical instability criterion, which was established in the early tokamaks and examined by recent numerical simulations.

Acknowledgment

This work has been carried out within the framework of the EUROFusion Consortium and has received funding from the EURATOM research and training programme 2014–2018 under grant agreement No 633053. IST activities also received financial support from "Fundação para a Ciência e Tecnologia" through project UID/FIS/50010/2013. A.E. Shevelev and E.M. Khilkevitch are grateful for financial support from the Ministry of Education and Science of the Russian Federation (Agreement No.14.619.21.0001, 15.08.2014, id RFMEFI61914X0001). The experiments on COMPASS were supported by the MEYS CR project No. LM2015045. The views and opinions expressed herein do not necessarily reflect those of the European Commission.

ORCID iDs

A. Kallenbach https://orcid.org/0000-0003-0538-2493
A.E. Shevelev https://orcid.org/0000-0001-7227-8448
O. Ficker https://orcid.org/0000-0001-6418-9517
A. Boboc https://orcid.org/0000-0001-8841-3309
M. Nocente https://orcid.org/0000-0003-0170-5275

References

[1] ITER Physics Basis 1999 Chapter 3: MHD stability, operational limits and disruptions *Nucl. Fusion* **39** 2251–389
[2] Hender T.C. *et al* and Progress in the ITER Physics Basis 2007 Chapter 3: MHD stability, operational limits and disruptions *Nucl. Fusion* **47** S178
[3] Giovanelli R.G. 1949 *Phil. Mag.* **40** 206–14
[4] Driecer H. 1959 *Phys. Rev.* **115** 238
[5] Dreicer H. 1960 *Phys. Rev.* **117** 329
[6] Harrison E.R. 1960 *J. Nucl. Energy* C **1** 105
[7] Harrison E.R. 1962 *J. Nucl. Energy* C **4** 7
[8] Jarvis O.N., Sadler G. and Thompson J.L. 1988 *Nucl. Fusion* **28** 1981
[9] Wesson J.A. *et al* 1989 *Nucl. Fusion* **29** 641
[10] Gill R.D. *et al* 2002 *Nucl. Fusion* **42** 1039
[11] Plyusnin V.V. *et al* 2006 *Nucl. Fusion* **46** 277
[12] Reux C. *et al* 2015 *Nucl. Fusion* **55** 093013
[13] Reux C. *et al* 2015 *Nucl. Fusion* **55** 129501
[14] Nygren R. *et al* 1997 *J. Nucl. Mater.* **241–3** 522
[15] Tamai H. *et al* 2002 *Nucl. Fusion* **42** 290
[16] Fredrickson E.D., Bell M.G., Taylor G. and Medley S.S. 2015 *Nucl. Fusion* **55** 013006
[17] Sokolov Yu.A. 1979 *JETP Lett.* **29** 218
[18] Besedin N.T. and Pankratov I.M. 1986 *Nucl. Fusion* **26** 807
[19] Rosenbluth M.N. and Putvinski S. V. 1997 *Nucl. Fusion* **37** 1355
[20] Plyusnin V.V. *et al* 2002 *Plasma Phys. Control. Fusion* **44** 2021–31
[21] Martin-Solis J.R. *et al* 2006 *Phys. Rev. Lett.* **97** 165002
[22] Smith H.M. and Verwichte E. 2008 *Phys. Plasmas* **15** 072502
[23] Aleynikov P. and Breizman B.N. 2017 *Nucl. Fusion* **57** 046009
[24] Putvinski S. *et al* 1997 *Plasma Phys. Control. Fusion* **39** B157
[25] Plyusnin V.V. *et al* 2012 Latest progress in studies of runaway electrons in JET *Paper presented 24th IAEA Fusion Energy Conference (San Diego, United States, 8–13 October 2012)* EX/P8-05 (http://www-naweb.iaea.org/napc/physics/FEC/FEC2012/papers/201_EXP805.pdf)
[26] Smith H. *et al* 2006 *Phys. Plasmas* **13** 102502
[27] Bazylev B. *et al* 2011 *J. Nucl. Mater.* **415** S841
[28] Hollmann E. M. *et al* 2013 *Nucl. Fusion* **53** 083004
[29] Lehnen M. *et al* 2013 *Nucl. Fusion* **53** 093007
[30] Papp G. *et al* Runaway electron generation and mitigation on the European medium sized Tokamaks ASDEX-upgrade and TCV *Preprint: 2016 IAEA Fusion Energy Conf. (Kyoto, Japan 17–22 October 2016)* EX/9-4 (https://nucleus.iaea.org/sites/fusionportal/Shared Documents/FEC 2016/fec2016-preprints/preprint0502.pdf)
[31] Mlynar J. *et al* 2017 Losses of runaway electrons in MHD-active plasmas of the COMPASS Tokamak 2017 *Nucl. Fusion* **57** 076002
[32] Martin P. *et al* Physics, control and mitigation of disruptions and runaway electrons in the EUROfusion medium size Tokamaks science programme *Preprint: 2016 IAEA Fusion Energy Conf. (Kyoto Japan 17–22 October 2016)* EX/P6-23 (https://nucleus.iaea.org/sites/fusionportal/Shared Documents/FEC 2016/fec2016-preprints/preprint0384.pdf)
[33] Plyusnin V.V. *et al* 2014 Parameters of runaway electrons in JET *25th IAEA Fusion Energy Conference (St Petersburg, Russia, 13–18 October 2014)* EX/P5-23 (www-naweb.iaea.org/napc/physics/FEC/FEC2014/fec2014-preprints/486_EXP523.pdf)
[34] Granetz R.S. *et al* 2014 *Phys. Plasmas* **21** 072506
[35] Plyusnin V.V. *et al* 2015 Parameters and stability of runaway electron dominating discharge in JET with ITER-like wall *42th EPS Conf. on Plasma Physics (ECA) (Lisbon, Portugal 22–26 June 2015)* vol 39E P2.127 (http://ocs.ciemat.es/EPS2015PAP/pdf/P2.127.pdf)
[36] Shevelev A. *et al* 2013 *Nucl. Fusion* **53** 123004
[37] Vlainic M. *et al* 2015 *J. Plasma Phys.* **81** 475810506
[38] Pestchanyi S. *et al* 2013 *Fusion Eng. Des.* **88** 1127–31
[39] Plyusnin V.V. and Pankratov I.M. 2011 Influence of three-dimensional plasma dynamics on runaway electron generation at major disruptions in Tokamaks *38th EPS Conf. on Plasma Physics (ECA) (Strasbourg, France, 27 June–1 July 2011)* vol 35G p P4.09 (http://ocs.ciemat.es/EPS2011PAP/pdf/P4.091.pdf)
[40] Mott N.F. and Massey H.S.W. 1965 *The Theory of Atomic Collisions* 3rd edn (Oxford: Clarendon)
[41] Rudge M.R.H. and Schwartz S.B. 1966 The ionization of hydrogen and of hydrogenic positive ions by electron impact *Proc. Phys. Soc.* **88** 563
[42] Aldrovandi S.M.V. and Pequignot D. 1973 *Astron. Astrophys.* **26** 33–43
[43] Heitler W. 1954 *The Quantum Theory of Radiation* 3rd edn (Oxford: Clarendon)
[44] Morozov D.Kh. *et al* 2007 *Plasma Phys. Rep.* **33** 906
[45] Lehnert B. 1968 *Nucl. Fusion* **8** 173
[46] Coppi B. *et al* 1975 Quasi-resistive regimes in magnetically confined plasmas *Phys. Lett.* **55A** 221
[47] Connor J. W. and Hastie R.J. 1975 *Nucl. Fusion* **15** 415
[48] Chiu S.C. *et al* 1998 *Nucl. Fusion* **38** 1711
[49] Besedin N.T., Kuznetsov Yu.K. and Pankratov I.M. 1986 *Sov. J. Plasma Phys.* **12** 436
[50] Jaspers R. *et al* 1993 *Nucl. Fusion* **33** 1775
[51] Pankratov I.M. *et al* 1998 *Nucl. Fusion* **38** 279
[52] Vlasenkov V.S., Leonov V.M., Merezhkin V.G. and Mukhovatov V.S. 1973 *Nucl. Fusion* **13** 509
[53] Alikaev V.V., Razumova K.A. and Sokolov Yu.A. 1975 *Sov. J. Plasma Phys.* **1** 303
[54] Hong-Wei L. *et al* 2010 *Chin. Phys.* B **19** 125201
[55] Chen Z.Y. *et al* 2011 *J. Korean Phys. Soc.* **59** 271
[56] Parail V.V. and Pogutse O.P. 1978 *Nucl. Fusion* **18** 303
Parail V.V. and Pogutse O.P. 1978 *Nucl. Fusion* **18** 1357
[57] Fuchs V., Shoucri M., Teichmann J. and Bers A. 1988 *Phys. Fluids* **31** 2221
[58] Aleynikov P. and Breizman B. 2015 Stability analysis of runaway-driven waves in a tokamak *Nucl. Fusion* **55** 043014
[59] Meyer H. *et al* 2017 *Nucl. Fusion* **57** 102014
[60] Litaudon X. *et al* 2017 *Nucl. Fusion* **57** 102001